Biomechan Model Mechanobiol (2007) 6: 21–32
DOI 10.1007/s10237-006-0045-y

ORIGINAL PAPER

T. J. Klein · R. L. Sah

Modulation of depth-dependent properties in tissue-engineered cartilage with a semi-permeable membrane and perfusion: a continuum model of matrix metabolism and transport

Received: 2 June 2005 / Accepted: 6 July 2005 / Published online: 20 May 2006

Abstract The functional properties of cartilaginous tissues are determined predominantly by the content, distribution, and organization of proteoglycan and collagen in the extracellular matrix. Extracellular matrix accumulates in tissue-engineered cartilage constructs by metabolism and transport of matrix molecules, processes that are modulated by physical and chemical factors. Constructs incubated under free-swelling conditions with freely permeable or highly permeable membranes exhibit symmetric surface regions of soft tissue. The variation in tissue properties with depth from the surfaces suggests the hypothesis that the transport processes mediated by the boundary conditions govern the distribution of proteoglycan in such constructs. A continuum model (DiMicco and Sah in Transport Porus Med 50:57–73, 2003) was extended to test the effects of membrane permeability and perfusion on proteoglycan accumulation in tissue-engineered cartilage. The concentrations of soluble, bound, and degraded proteoglycan were analyzed as functions of time, space, and non-dimensional parameters for several experimental configurations. The results of the model suggest that the boundary condition at the membrane surface and the rate of perfusion, described by non-dimensional parameters, are important determinants of the pattern of proteoglycan accumulation. With perfusion, the proteoglycan profile is skewed, and decreases or increases in magnitude depending on the level of flow-based stimulation. Utilization of a semi-permeable membrane with or without unidirectional flow may lead to tissues with depth-increasing proteoglycan content, resembling native articular cartilage.

T. J. Klein · R. L. Sah (✉)
Department of Bioengineering, University of California,
San Diego, 9500 Gilman Dr., Mail Code 0412, La Jolla,
CA 92093-0412, USA
E-mail: rsah@ucsd.edu
Tel.: +1-858-5340821
Fax: +1-858-8221614

R. L. Sah
Whitaker Institute of Biomedical Engineering,
University of California, San Diego, La Jolla, CA, USA

1 Introduction

Adult articular cartilage is an avascular tissue that lines the ends of long bones and functions as an efficient load-bearing surface in synovial joints (Buckwalter and Mankin 1997; Mow et al. 1991). Chondrocytes are sparsely distributed in a hydrated extracellular matrix consisting mostly of collagens (predominantly type II) and proteoglycans (primarily aggrecan). When matrix macromolecules are secreted by a chondrocyte, they are initially soluble and able to diffuse. They may then be bound to the existing matrix, transported out of the local region of cartilage tissue, or degraded by enzymes such as matrix metalloproteinases (MMPs) or aggrecanases (Arner et al. 1999). During normal function, chondrocytes are able to balance synthesis, deposition, and degradation of matrix molecules to maintain homeostasis. Normally, articular cartilage exhibits proteoglycan content that increases with depth and contributes in large part to a depth-associated increase in compressive modulus (Chen et al. 2001; Schinagl et al. 1997). Alterations in synthesis, binding, and degradation all may play a part in disrupting the balance and lead to changes in cartilage composition and function. During cartilage development and growth, the metabolic balance favors anabolism, and tissue accumulates. After injury or with disease, the balance can be shifted to favor catabolism, and components of the cartilage matrix are lost, as are the functional properties of the tissue (Buckwalter and Mankin 1998).

The frequent damage and ineffective intrinsic repair response of articular cartilage has led to investigations into treatment modalities involving engineered tissues. Here, cells and materials are combined, then incubated under various conditions to form cartilaginous tissues, which could serve as implants for replacing areas of damaged cartilage (Sah et al. 2004). Attempts to grow cartilaginous tissues in vitro using standard static tissue-culture methods have been hampered by transport limitations. These problems are exemplified by cell death and lack of matrix accumulation at the center of the constructs (Heywood et al. 2004; Pei et al. 2002), possibly due to a lack of nutrients, or an overabundance of waste

products at the center of the tissue. Bioreactor culture systems have been developed to overcome these limitations with the aid of fluid flow (Vunjak-Novakovic et al. 2002; Li et al. 2004). Different types of bioreactors can generate diverse types of fluid flow: rotating-wall vessels generally induce flow at the tissue surfaces (Freed et al. 1997); compressive loading chambers induce non-steady flow at the periphery (Mauck et al. 2000); and direct perfusion chambers force flow through the constructs (Dunkelman et al. 1995; Pazzano et al. 2000; Davisson et al. 2002). The benefits of fluid flow are numerous, including improvement of mass transfer (Obradovic et al. 1999), and metabolic stimulation (Davisson et al. 2002).

Several models of varying complexity have been used to describe the metabolism and matrix deposition of cartilaginous tissues in vitro. The simplest model considered the average concentration of proteoglycan in the tissue as a function of time to depend on synthesis and degradation rates, and to result in steady-state metabolism (Hascall et al. 1990). While this model can account for overall matrix homeostasis, it attempts neither to describe transport mechanisms, nor depth-varying tissue properties. Diffusion-reaction models have been developed to elucidate spatial, as well as temporal information (Obradovic et al. 2000; DiMicco and Sah 2003). In one model, oxygen concentration and proteoglycan production were coupled to explain time- and depth-dependent patterns of proteoglycan accumulation in constructs cultivated in rotating-wall biorectors (Obradovic et al. 2000). An alternative model described the development of spatially-dependent matrix properties of articular cartilage by considering the synthesis, binding, transport, and interaction of matrix molecules (DiMicco and Sah 2003). With modifications, such a model may give insight into the role of fluid flow and boundary conditions on matrix accumulation in engineered tissues.

Tissue-engineered cartilage constructs have been fabricated with a variety of boundary conditions, with apparent effects on proteoglycan accumulation. Constructs grown in free-swelling culture, or rotating-wall bioreactors, are in direct contact at all tissue surfaces with the culture medium. The resultant tissues typically have a thin region at the surface that does not stain for proteoglycan with safranin-O (Pei et al. 2002), consistent with free diffusion of proteoglycans from the boundaries (Obradovic et al. 2000). Other constructs have been formed by confining a cell suspension with one or two semi-permeable membranes in vivo (Haddo et al. 2004), or in vitro (Grogan et al. 2003). Depending on the properties of the membrane (i.e., permeability, reflection coefficient), particles ranging in size from cells to macromolecules can be retained. Tissues formed between ultrafiltration membranes to retain macromolecules (>0.1 MDa), stained uniformly with safranin-O (Grogan et al. 2003), consistent with no-flux boundary conditions for proteoglycan at both surfaces. Constructs formed by layering alginate-recovered chondrocytes (Mauck et al. 2003) from the superficial and middle/deep zones onto a highly-permeable membrane (Klisch et al. 2003) exhibited soft regions at both surfaces, as did constructs formed by mixing chondrocytes from the different zones (Klein 2005). Since these constructs were incubated with a permeable basal membrane, the spatial variation in tissue properties may have been due to unhindered transport at both surfaces.

The aims of this study were to extend a continuum model of matrix metabolism and transport (DiMicco and Sah 2003) to model the temporal and spatial proteoglycan accumulation in tissue-engineered cartilage. One aim was to incorporate a variable basal boundary condition, to determine effects of varying membrane properties on the distribution of proteoglycan in constructs. An additional aim was to assess effects of perfusion based solely on transport processes, or on both transport and biosynthesis rates.

2 Continuum model

2.1 Model overview

A continuum model of the time- and space-dependent accumulation of proteoglycan in tissue-engineered cartilage is developed by extending a previous model of matrix accumulation in articular cartilage cultured with free-swelling conditions (DiMicco and Sah 2003) to consider effects of perfusion and membrane boundary conditions. This model considers proteoglycan molecules to be in one of three pools: soluble (s), bound (b), or degraded (d) (Fig. 1). A mass balance is used to generate governing equations for each of the pools. Proteoglycan is synthesized at a volumetric rate of formation [r_f, g/(cm^3 s)], bound to existing matrix at a volumetric rate of binding [r_b,g/(cm^3 s)], and bound molecules are degraded at a volumetric rate of degradation [r_d, g/(cm^3 s)]. The soluble and degraded molecules are considered to be able to diffuse, with specific diffusivities (D_s, D_d, cm^2/s), and to be transported by convection with an average perfusion velocity over the construct area (v, cm/s). The soluble and degraded proteoglycan concentrations are assumed to be equal to the concentration in the medium at free surfaces, while bound proteoglycan flux across these surfaces is assumed to be zero. At the membrane surface, a flux balance is used to determine the boundary condition, accounting for the membrane permeability (w, cm/s), and variable reflection coefficients for soluble and degraded proteoglycan (σ_s, σ_d, dimensionless). The model considers only variations in the axial dimension and time. Variations in the radial direction are not accounted for, but are expected to be comparatively small for fairly uniform velocity profiles. Also, although the concentration of matrix molecules is allowed to vary with depth, the construct is assumed to have a constant thickness (h, cm), and constant transport properties. A complete list of symbols used in the model is given in Table 1.

2.2 Governing equations

The governing equations for the concentration of soluble (c_s), bound (c_b), and degraded (c_d) proteoglycan in the construct ($z = 0 - h$) are obtained from a molecular mass balance,

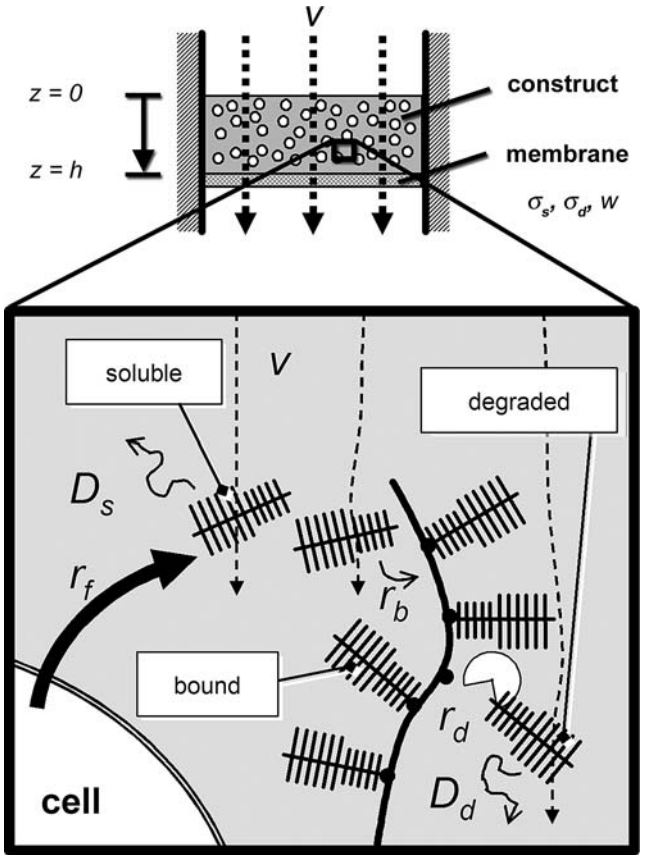

Fig. 1 Schematic of continuum model, (adapted from DiMicco and Sah 2003). A tissue-engineered construct seated on top of a semi-permeable membrane is perfused with medium, while synthesis, transport, binding, and degradation of proteoglycan occur. Macromolecules are modeled as soluble, bound, or degraded, and the locations of action for the various model parameters used in the governing equations (1–3), and boundary conditions (10, 11, 14, 15), are indicated by their placement in the figure. See Table 1 for a complete list of variables

and account for reaction (r terms), diffusion (D terms), and perfusion (v terms).

Proteoglycan molecules synthesized by the chondrocytes at a particular rate (r_f) are added to the soluble pool, and are considered mobile (may be transported by convection or diffusion), until they are bound to existing matrix, at a particular rate (r_b), or are transported out of the tissue. If a constant perfusion velocity is assumed throughout the construct (v), the change in soluble concentration with time is governed by

$$\frac{\partial c_\mathrm{s}}{\partial t} = r_\mathrm{f} - r_\mathrm{b} + D_\mathrm{s}\frac{\partial^2 c_\mathrm{s}}{\partial z^2} - v\frac{\partial c_\mathrm{s}}{\partial z}. \tag{1}$$

Molecules enter the bound pool from the soluble pool by binding to existing matrix, and are lost from this pool by degradation, at a rate, r_d. Since bound molecules are assumed to be immobilized, the governing equation is

$$\frac{\partial c_\mathrm{b}}{\partial t} = r_\mathrm{b} - r_\mathrm{d}. \tag{2}$$

Degraded molecules are considered to be mobile, and unable to bind to the existing matrix. Thus, the change in concentration of degraded molecules with time is

Table 1 List of variables

Variables	Description	Units
z	Position	cm
t	Time	s
v	Perfusion velocity	cm/s
h	Thickness	cm
c_s	Soluble concentration	g/cm^3
c_b	Bound concentration	g/cm^3
c_d	Degraded concentration	g/cm^3
c_tot	Total concentration	g/cm^3
c_0	Tissue density	g/cm^3
c_b0	Initial bound concentration	g/cm^3
k_f	Formation rate constant	s^{-1}
k_b	Binding rate constant	s^{-1}
k_d	Degradation rate constant	s^{-1}
r_f	Volumetric synthesis rate	g/(cm^3 s)
r_b	Volumetric binding rate	g/(cm^3 s)
r_d	Volumetric degradation rate	g/(cm^3 s)
D_s	Soluble diffusivity	cm^2/s
D_d	Degraded diffusivity	cm^2/s
b	Perfusion synthesis parameter	g/cm^2
w	Membrane permeability	cm/s
J_s	Flux of soluble molecules	g/(cm^2 s)
α	Non-dimensional synthesis parameter	
β	Non-dimensional perfusion parameter	
δ	Non-dimensional perfusion synthesis parameter	
λ_s	Non-dimensional membrane parameter (soluble)	
λ_d	Non-dimensional membrane parameter (degraded)	

$$\frac{\partial c_\mathrm{d}}{\partial t} = r_\mathrm{d} + D_\mathrm{d}\frac{\partial^2 c_\mathrm{d}}{\partial z^2} - v\frac{\partial c_\mathrm{d}}{\partial z}. \tag{3}$$

2.3 Reaction rates

The reaction rates can be functions of time and space, and are considered to be dependent on the local concentrations of the molecules in specific pools. Here, it is assumed that there is a basal synthesis rate (Hascall et al. 1990; DiMicco and Sah 2003), given by the rate of formation constant (k_f, s^{-1}) multiplied by the density of material in the construct (c_0, g/cm^3). Biosynthesis may also be dependent on perfusion velocity (Davisson et al. 2002), and this is described by a perfusion rate constant [b, g/(cm^4)] that relates the additional volumetric synthesis per change in velocity. Thus, the rate of formation used is

$$r_\mathrm{f} = k_\mathrm{f} c_0 + bv \tag{4}$$

This rate law can be simplified under the assumption that the perfusion rate constant (b) is zero, to yield a constant rate of formation, as is assumed for cartilage explant cultures.

The rate of binding is dependent on the concentration of molecules that are able to bind. It is assumed that only soluble molecules may bind (Arner et al. 1999), and that the rate is proportional to the soluble concentration (c_s):

$$r_\mathrm{b} = k_\mathrm{b} c_\mathrm{s}. \tag{5}$$

The rate of degradation is dependent on the concentration of molecules that can degrade. Here, it is assumed that

only the bound molecules can degrade, with a degradation rate constant (k_d, s^{-1}):

$$r_d = k_d c_b. \tag{6}$$

By substituting the expanded rate laws (4–6) into Eqs. (1–3), the governing equations become:

$$\frac{\partial c_s}{\partial t} = k_f c_0 + bv - k_b c_s + D_s \frac{\partial^2 c_s}{\partial z^2} - v\frac{\partial c_s}{\partial z}, \tag{7}$$

$$\frac{\partial c_b}{\partial t} = k_b c_s - k_d c_b, \tag{8}$$

$$\frac{\partial c_d}{\partial t} = k_d c_b + D_d \frac{\partial^2 c_d}{\partial z^2} - v\frac{\partial c_d}{\partial z}. \tag{9}$$

The total concentration (c_{tot}, g/cm^3) is given by the sum of the soluble, bound, and degraded concentrations.

2.4 Boundary conditions

The boundaries of the construct are located at $z = 0$ (free surface) and $z = h$ (membrane surface). The tissue is in direct contact with the culture medium at the free surface. The concentration of proteoglycan in culture medium ranges from 0 to 0.015 mg/cm^3 during culture of certain constructs, whereas the average concentration in the tissue is 20 mg/cm^3 (Klein 2005). Thus, the concentrations of soluble and degraded matrix molecules in the medium are expected to be small relative to the concentrations in the constructs, and are assumed to be equal to 0. Since the soluble and degraded molecules are free to diffuse, the concentration in the tissue immediately below the free surface ($z = 0^-$), and in the medium immediately above the free surface ($z = 0^+$) will be the same. Hence, the soluble and degraded concentrations are constrained to be zero at $z = 0$:

$$c_s(0, t) = c_d(0, t) = 0. \tag{10}$$

The bound molecules, however, are not free to diffuse or convect, and thus may build up at the surfaces despite a zero concentration in the medium. The flux of bound molecules should be zero across the top and bottom surfaces:

$$\frac{\partial c_b}{\partial z}(0, t) = \frac{\partial c_b}{\partial z}(h, t) = 0. \tag{11}$$

The boundary conditions for the soluble molecules at the membrane surface ($z = h$) are dependent on the membrane properties, and may be determined by balancing the fluxes (J_s) in the tissue directly above the membrane ($z = h^-$) and just inside the membrane ($z = h^+$). Near the membrane, the flux is assumed to be convective and diffusive, as it is throughout the tissue:

$$J_s(h^-, t) = -D_s \frac{\partial c_s}{\partial z}(h^-, t) + v c_s(h^-, t). \tag{12}$$

In the membrane, there are convection and diffusion-like terms, as well. Since the membrane is selective, there is an additional factor, $(1 - \sigma_s)$, where σ_s is the reflection coefficient, that varies from 0 (unhindered transport) to 1 (molecule unable to pass) (Blanch and Clark 1996) (Fig. 2). The convective flux is given by the product of velocity and concentration. The diffusive flux of the soluble molecules can be described as the product of the membrane permeability (w, cm/s), and the difference in concentration between the construct at the membrane, $c_s(h, t)$, and the concentration in the medium (which is assumed to be 0):

$$J_s(h^+, t) = (1 - \sigma_s) \cdot (w c_s(h^+, t) + v c_s(h^+, t)). \tag{13}$$

By equating the fluxes at the membrane, the boundary condition for the soluble molecules is obtained:

$$\frac{\partial c_s}{\partial z}(h, t) = \frac{\sigma_s v - (1 - \sigma_s) w}{D_s} c_s(h, t). \tag{14}$$

The boundary condition for the degraded molecules at $z = h$ follows the same reasoning, with the only differences being the constants:

$$\frac{\partial c_d}{\partial z}(h, t) = \frac{\sigma_d v - (1 - \sigma_d) w}{D_d} c_d(h, t). \tag{15}$$

With no perfusion ($v = 0$) and an impermeable membrane ($w = 0$), the right-hand side reduces to zero, which is the expected boundary condition for a wall. If the construct is perfused, but the membrane remains impermeable to the soluble and degraded proteoglycan ($\sigma_s = \sigma_d = 1$), there will be a buildup of molecules at the surface of the membrane (Fig. 2b). A non-zero permeability and reflection coefficient of less than 1 allow for the release of molecules into the medium at $z = h$. If the reflection coefficient is low enough, reduced concentrations will be established at the membrane.

If the membrane is sufficiently permeable to allow proteoglycan to freely convect and diffuse across the membrane, the boundary conditions for the soluble and degraded molecules will be the same as at the top surface:

$$c_s(h, t) = c_d(h, t) = 0. \tag{16}$$

2.5 Initial conditions

The initial conditions can generally be a function of depth, but for simplicity are assumed to be constant throughout the tissue, with an initial bound concentration (c_{b0}, g/cm^3):

$$c_s(z, 0) = 0 \tag{17}$$

$$c_b(z, 0) = c_{b0} \tag{18}$$

$$c_d(z, 0) = 0. \tag{19}$$

2.6 Non-dimensional equations

The governing equations and boundary conditions can be non-dimensionalized by defining non-dimensional length, time, and concentrations:

$$z' = \frac{z}{h}. \tag{20}$$

$$t' = \frac{t D_s}{h^2}. \tag{21}$$

$$c_i' = \frac{c_i}{c_0}; \quad i = s, b, d. \tag{22}$$

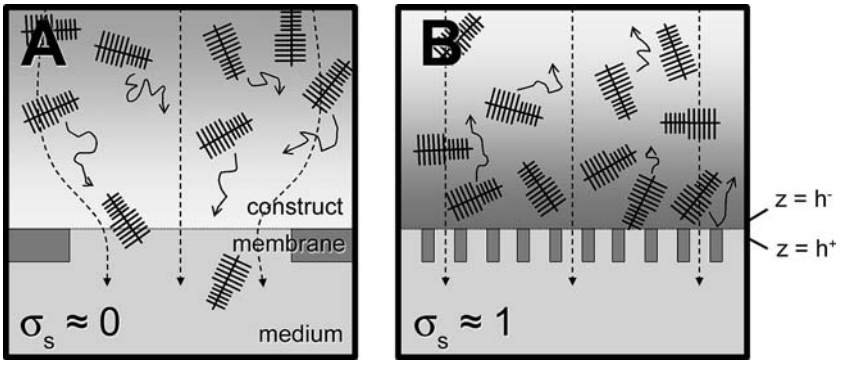

Fig. 2 Schematic of soluble proteoglycan transport near the membrane boundary of a cartilaginous construct. In **a**, the membrane has a low reflection coefficient (σ_s), and allows for transport of proteoglycan by diffusion (*random paths*) or convection (*dashed line*), leading to a low concentration (*light shading*) near the construct surface ($z = h$). In **b**, the membrane has a high reflection coefficient, hindering transport of proteoglycan from the construct to the medium. With perfusion, a buildup of proteoglycan occurs at the membrane, combated by diffusion of molecules back into the tissue

After substitution, and simplification, the non-dimensional governing equations become:

$$\frac{\partial c_s'}{\partial t'} = \alpha\left(1 - \frac{k_b}{k_f}c_s'\right) + \frac{\partial^2 c_s'}{\partial z'^2} - \beta\left(\frac{\partial c_s'}{\partial z'} - \delta\right), \tag{23}$$

$$\frac{\partial c_b'}{\partial t'} = \alpha\left(\frac{k_b}{k_f}c_s' - \frac{k_d}{k_f}c_b'\right) \tag{24}$$

$$\frac{\partial c_d'}{\partial t'} = \alpha\frac{k_d}{k_f}c_b' + \frac{D_d}{D_s}\frac{\partial^2 c_d'}{\partial z'^2} - \beta\frac{\partial c_d'}{\partial z'} \tag{25}$$

Non-dimensional parameters α, β, and δ are defined as:

$$\alpha = \frac{h^2 k_f}{D_s}, \quad \beta = \frac{hv}{D_s}, \quad \delta = \frac{bh}{c_o}. \tag{26}$$

The non-dimensional synthesis parameter, α, which is the square of the Thiele modulus, relates the rate of formation to the rate of diffusion. The non-dimensional perfusion parameter, β, which is a Peclet number, relates the rate of convective mass transfer to the rate of diffusive mass transfer. Finally, the non-dimensional perfusion synthesis parameter, δ, is an estimate of the relative effects of perfusion on stimulation of synthesis.

The non-dimensional boundary conditions are:

$$c_s'(0, t') = c_d'(0, t') = 0, \tag{27}$$

$$\frac{\partial c_b'}{\partial z'}(0, t') = \frac{\partial c_b'}{\partial z'}(1, t') = 0, \tag{28}$$

$$\frac{\partial c_s'}{\partial z'}(1, t') = (\sigma_s\beta - \lambda_s)c_s'(1, t'), \tag{29}$$

$$\frac{\partial c_d'}{\partial z'}(1, t') = \left(\frac{D_s}{D_d}\sigma_d\beta - \lambda_d\right)c_d'(1, t'). \tag{30}$$

The non-dimensional boundary conditions introduce a non-dimensional membrane parameter for the soluble and degraded molecules:

$$\lambda_s = \frac{(1 - \sigma_s)wh}{D_s}, \quad \lambda_d = \frac{(1 - \sigma_d)wh}{D_d}. \tag{31}$$

This parameter compares the diffusive transport through the membrane and inside the tissue, and is equal to zero for a membrane that is impermeable to the molecules.

The non-dimensional initial conditions are

$$c_s'(z', 0) = 0, \quad c_b'(z', 0) = \frac{c_{b0}}{c_0}, \quad c_d'(z', 0) = 0. \tag{32}$$

2.7 Solutions

The initial-boundary value problems were solved numerically using Matlab 7.0 (The MathWorks, Natick, MA). Non-dimensional parameters were varied to determine the temporal and spatial effects of perfusion (β, δ, α), in a range where diffusion and convection effects are similar, and membrane properties (λ_s, λ_d), in a range from impermeable to permeable, on proteoglycan accumulation in tissue-engineered cartilage constructs. Parameter values for rate constants and diffusivities for proteoglycans were based on the literature values (DiMicco and Sah 2003) and are listed in Table 2. All plots are of non-dimensional concentrations versus non-dimensional depth or time. Equilibrium profiles were verified with analytical solutions of the non-dimensional governing equations (23–25), using Mathematica 5.1 (Wolfram Research, Inc., Champaign, IL). The form of the equilibrium profiles is:

$$c_s'(z, \infty) = e^{-2Bz}\left(A_1 - A_2 e^{Bz} + A_3 e^{2Bz} - A_4 e^{3Bz}\right) \tag{33}$$

$$c_b'(z, \infty) = \frac{k_b}{k_d}c_s'(z, \infty) \tag{34}$$

$$c_d'(z, \infty) = -c_s'(z, \infty) + \left(A_5 + A_6 e^{-Bz} + A_7 e^{Bz}\right)z - A_8 z^2, \tag{35}$$

where the A_i s and B are constants determined by the boundary conditions and non-dimensional parameters.

3 Results

3.1 Time-dependent proteoglycan distribution

To compare the evolution of proteoglycan accumulation in constructs with different boundary conditions, the time course of proteoglycan distribution in constructs with or without a membrane was modeled (Fig. 3). The free surface boundary conditions (27) were applied at the surfaces of the construct without a membrane (Fig. 3a–d), whereas the impermeable membrane condition [(29, 30), with $\lambda_s = \lambda_d = 0$] was applied at the membrane surface of the other construct (Fig. 3e–h). The construct cultured without a membrane rapidly developed a steady-state flattened-parabolic profile of soluble components (Fig. 3a), while the construct with a membrane developed a profile of increasing content with increasing depth, similar to the profile from $z' = 0 to 0.5$ of the no-membrane construct (Fig. 3e). The bound and degraded pools developed similar-shaped profiles, but were much slower in reaching equilibrium. The majority of the proteoglycan at equilibrium was in the bound form, with only a small percentage (~3% for no-membrane, ~7% for membrane) of the total content being degraded. The overall average content reached equilibrium at ~40 mg/cm^3 for the chosen parameter values, similar to values of articular cartilage (Sah et al. 1994) and certain constructs (Riesle et al. 1998).

3.2 Effects of perfusion

The transport- and stimulatory-based effects of perfusion on the equilibrium proteoglycan profiles of cartilage constructs were modeled by varying the non-dimensional perfusion parameter, β, for constant values of the non-dimensional perfusion synthesis parameter, δ, or non-dimensional synthesis parameter, α (Fig. 4). With increasing β, the concentration profile of the construct without a membrane shifted to the right, and decreased in magnitude (Fig. 4a–d). The degraded pool was most dramatically affected by changes in the perfusion parameter (Fig. 4c). When stimulatory effects of perfusion were incorporated ($\delta = 0.001$), the profiles remained right-shifted, but generally increased in magnitude (Fig. 4e–h), indicating the stimulatory effect was outweighing the transport effects. The profiles of soluble and bound components were quite different when an impermeable membrane ($\lambda_s = \lambda_d = 0$) was present at the bottom of the construct (Fig. 4i–p). With increasing β, the gradient became flattened near the top of the construct, but in the bottom quarter of the construct there was a dramatic increase in concentration, consistent with the filtering behavior of the membrane. This concentration polarization effect is realistically limited by the formation of a gel layer at concentration of ~0.1–0.3 g/cm^3, at which point the concentration cannot increase further (Blanch and Clark 1996). Such a layer would increase the pressure needed to drive the fluid through the construct and membrane. The diffusivity of the soluble component was assigned high (10^{-8} cm^2/s, Fig. 4i–l) or low (10^{-9} cm^2/s, Fig. 4m–p) values to determine its relative effect on profiles with changes in β. For the same range of β (but different α), there was reduced accumulation near the membrane, and a more flattened profile (Fig. 4j–l).

3.3 Effects of membrane properties

The non-dimensional membrane parameters, λ_s and λ_d, were varied to test the hypothesis that the soft surfaces of statically cultured layered constructs was due to transport through the membrane surface (Klein 2005). Without flow, decrease of λ_s and λ_d to zero was predicted to change the proteoglycan concentration from symmetric (as in Fig. 4a–d), to asymmetric, with a higher concentration at the basal surface than at the free surface (as in Fig. 4e–f). The boundary conditions at $z'=1$ were as in Eqs. 30 and 31, and the non-dimensional membrane parameters (λ_s, λ_d), were varied from 0.17 to 1.7 $\times$ 10^3 in a logarithmic fashion. With increases in these parameters, the equilibrium profiles in a non-perfused construct (Fig. 5a–d) progressed from semi-parabolic (similar to Fig. 4e–h) to parabolic (similar to Fig. 4 a–d). For large values of λ_s and λ_d, the concentrations matched those of constructs treated with the free surface boundary condition. When flow was applied to simulate culture under perfused conditions (Fig. 5e–h), the profiles varied from maximum accumulation near the membrane, to right-shifted profiles (similar to Fig. 4a–d).

4 Discussion

This study has established a theoretical basis for the effect of culturing cartilaginous tissues with a semi-permeable membrane, with or without unidirectional perfusion, on depth-varying proteoglycan content. A boundary condition describing variable membrane permeability was added to a previous continuum model (DiMicco and Sah 2003) to account for realistic properties of membranes used in construct cultures. The results indicate that constructs grown in static culture on a highly-permeable membrane will develop a symmetric proteoglycan profile with depth (Fig. 3a–d), whereas constructs cultured with reduced permeability membranes will show an increase in content with depth from the free surface (Fig. 3e–h, 5a–d). Addition of flow to these cultures also generates asymmetric concentration profiles, while reducing overall content (Fig. 4a–d), unless stimulatory effects of perfusion are included (Fig. 4e–h). Several non-dimensional parameters were identified, each with distinct effects on the pattern of proteoglycan accumulation, which could be useful when designing culture systems to engineer cartilaginous tissues with depth-dependent properties.

While the model can account for observed and expected changes in tissue composition under different culture conditions, there were several assumptions that should be considered when interpreting the results. Although the concentration of proteoglycan was allowed to vary with depth,

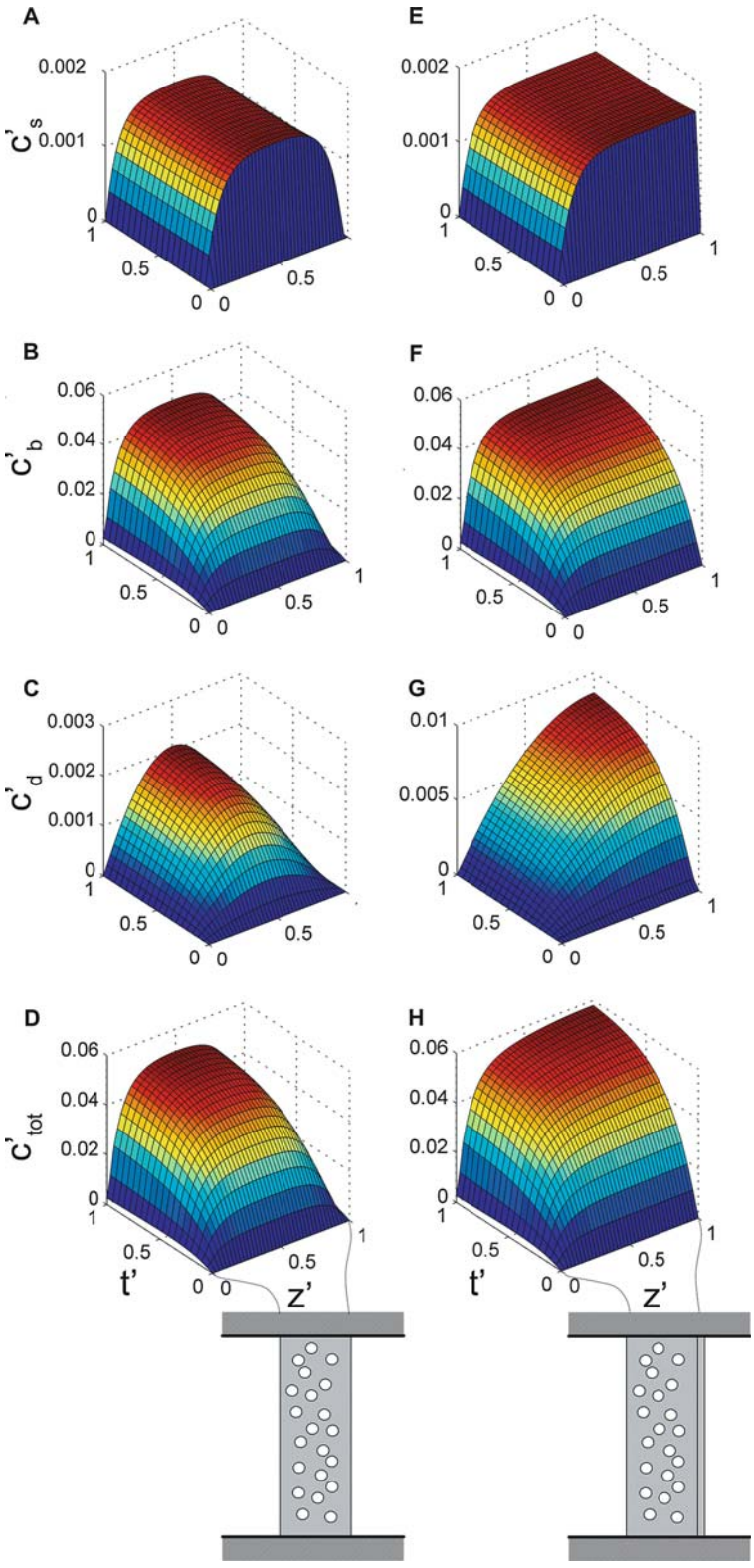

Fig. 3 Time- and depth-dependent normalized concentration profiles of **a** and **e** soluble, **b** and **f** bound, **c** and **g** degraded, and **d** and **h** total molecules in constructs **a–d** without or **e–h** with a membrane that is impermeable to soluble and degraded proteoglycan ($\sigma_s = \sigma_d = 0$ at $z' = 1$). Initial concentrations of 0 were used for all pools, and no perfusion was applied

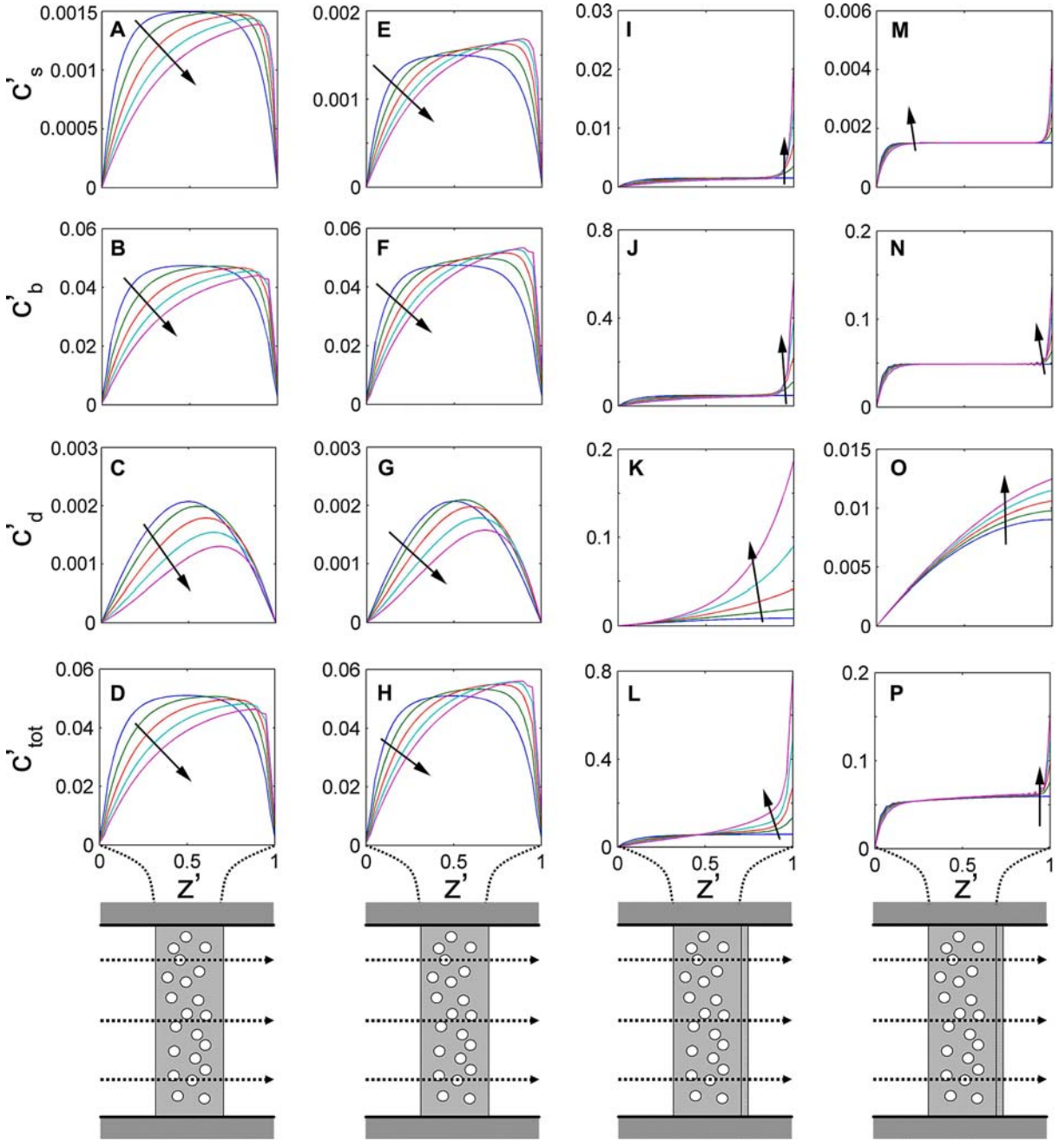

Fig. 4 Equilibrium normalized concentration profiles of soluble, bound, degraded, and total molecules as a function of non-dimensional perfusion parameter, β, which ranged linearly from 0 to 4 (increasing in direction of the *arrow*). Concentration profiles for constructs without a membrane, with **a–d** no metabolic effect of perfusion, and **e–h** a stimulatory response to perfusion are shown. Also, profiles for constructs with a membrane are shown with **i–1** the standard soluble diffusivity or **m–p** or an order of magnitude reduced soluble diffusivity (and an order of magnitude reduced velocity), while keeping the degraded diffusivity unchanged

the physical properties of the construct (e.g., thickness and diffusivity) were assumed to be constant in space and time. The constant geometry assumption is valid for several types of cartilage, and is reasonable for many engineered constructs with pre-formed dimensions, but may not be appropriate for constructs that increase in thickness with culture duration (Klisch et al. 2003). At later time points, however, such constructs maintain constant thickness, and may be more appropriately modeled. A moving boundary layer approach could be used to account for changes in dimensions when modeling growing tissues (Galban and Locke 1997). The diffusivity, while assumed constant in this model, likely will vary as matrix is accumulated, as zonal variations in diffusivity are present in articular cartilage (Leddy and Guilak 2003).

Table 2 Values used in the model

Variable	Value	Units	Figures	References
k_f	1.9×10^{-8}	s^{-1}		Sah et al. (1994)
k_b	1.2×10^{-5}	s^{-1}		Sandy et al. (1989)
K_d	3.7×10^{-7}	s^{-1}		Sandy and Plaas (1986)
v	$0–4\times10^{-7}$	cm/s	4, 5	
b	0 or 0.01	g/cm^4	4a–h	
D_s	10^{-8} or 10^{-9}	cm^2/s	4i–p	Comper and Williams (1987) and Leddy et al. (2004)
D_d	10^{-8}	cm^2/s		DiMicco and Sah (2003) and Leddy et al. (2004)
w	1.7×10^{-4}	cm/s		
h	0.1	cm		Klisch et al. (2003)
c_0	1.0	g/cm^3		
C_{b0}	0	g/cm^3		
σ_s	0–1		5	
σ_d	0–1		5	
α	0.019–0.19		4i–p	
β	0–4		4	
δ	0–0.001		4a–h	
λ_s	$0–1.7\times10^3$		5	
λ_d	$0–1.7\times10^3$		5	

Such changes would tend to reduce the diffusion length, thereby altering the proteoglycan profiles. An example of this effect is shown by an order of magnitude change in diffusivity (Fig. 4i, m). In addition to affecting the non-dimensional perfusion parameter, β, the diffusivity affects the synthesis parameter, α. Thus, it has complex effects on the accumulation of proteoglycan. While accounting for time- and depth-dependent diffusivity may be a useful addition to the model, large molecules (0.5 MDa dextran) have displayed fairly constant diffusivity over the first four weeks of construct culture (Leddy et al. 2004). The rate laws could be further refined to account for experimental observations of synthesis inhibition or promotion due to the presence of intact (Wilson et al. 2002; Buschmann et al. 1992), or degraded (Jennings et al. 2001) molecules.

The mechanical properties resulting from different culture conditions were not analyzed specifically, but are likely to be related to the biochemical content of the matrix, as well as its organization (Mow and Guo 2002). Other models have investigated the development of mechanical properties in growing cartilage with changes in proteoglycan, collagen, and water content, and have posited that the mode of growth or maturation is also an important consideration, as molecular concentrations may not increase during expansive growth, but would increase in maturational growth (Klisch et al. 2003). Formation of an anisotropic collagen network, with fiber orientation ranging from parallel to the articular surface in the superficial zone, to perpendicular to this surface in the deep zone, cannot be accounted for in the present model, but is expected to have importance in both natural development and development of mechanical properties of constructs. Such anisotropic properties have been modeled in the context of tissue growth under deformational loading, with Wolff-type laws governing the orientation and size of growing fibers (Menzel 2005). Solid deformation was not directly applied to the construct in the present model, but small amounts of compression are likely to occur with the application of fluid flow (Mow et al. 1999).

The results of this model suggest that perfusion can have net positive or negative effects on matrix deposition in cartilaginous constructs, depending on the perfusion rate and the metabolic response. In all simulations except for those in Fig. 4e–h, applied flow was only used as a mechanism of transport, by varying the non-dimensional perfusion parameter, β. The profiles for $\beta > 0$ changed in shape with respect to the static constructs. The overall concentration was also reduced due to convective loss of soluble and degraded molecules (Fig. 4a–d), contrary to existing data in the literature that generally associates perfusion with increases in proteoglycan content (Raimondi et al. 2004; Dunkelman et al. 1995; Davisson et al. 2002; Pazzano et al. 2000). However, when the anabolic influence of perfusion on biosynthesis rate was accounted for, by increasing the value of the non-dimensional perfusion synthesis parameter (δ), the proteoglycan content increased, overcoming the convective loss (Fig. 5e–h). Depending on the design of the bioreactor, the flow profile may range from constant to parabolic in the radial direction. If the flow significantly varies with construct radius, two-dimensional analysis using cylindrical coordinates would be needed.

The model analysis of the effects of perfusion could be refined, with additional information on the mechanisms of perfusion effects on cell and tissue metabolism. For example, shear stress and hydrostatic pressure are applied to the chondrocytes during perfusion (Davisson 2001), both of which have been implicated in metabolic regulation (Smith et al. 2004). Shear stress increases intracellular calcium in chondrocytes (Yellowley et al. 1999), and synthesis of inflammatory and matrix molecules (Smith et al. 1995). Hydrostatic pressure has been shown to increase synthesis of matrix and tissue inhibitor of metalloproteinases (Trindade et al. 2004). Thus, the mechanical factors in perfusion culture could affect

not only the synthesis rate, but also the degradation rate, and ultimately the amount of retained matrix (Gooch et al. 2001; Mizuno et al. 2002). If the anabolic effects of perfusion are not enough to overcome the convective loss, supplementation of the culture medium with a growth factor (modeled as an increase in α) may be sufficient to favor matrix accumulation, or may even act synergistically with the mechanical factors (Mauck et al. 2003).

The use of a semi-permeable membrane during construct culture can also have major effects on the matrix properties with depth, and is amenable to culture with perfusion. The selection of an appropriate membrane pore size is important to consider when designing a bioreactor for cultivating tissues with specific depth-dependent properties. In one case, membranes with 0.4 μm pore size (Klisch et al. 2003), which will filter out molecules of greater than ~40 MDa, have been used to engineer cartilage constructs. While this membrane is appropriate for retaining cells, it is too coarse to retain aggrecan monomers (~3 MDa (Comper and Williams 1987)) or newly synthesized procollagen [~0.5 MDa (Church et al. 1971)]. Membranes with a molecular weight cutoff of <0.5 MDa may be beneficial for retention of these macromolecules, while allowing for efficient transport of nutrients. Such membranes (0.1 MDa molecular weight cutoff) have been applied to both construct surfaces in static culture, resulting in uniform proteoglycan deposition throughout the tissue (Grogan et al. 2003). The current model suggests that tissues grown with membranes at both surfaces should develop a uniform proteoglycan distribution in the absence of perfusion. Careful selection of the membrane pore size may allow for retention of newly synthesized molecules, while allowing for release of degradation products that may negatively influence chondrocyte metabolism and ultimately construct function. Constructs cultured with either one or two membranes, and confined at the periphery by either a cell culture insert, or custom chamber (Grogan et al. 2003), could allow for ease of construct transfer from an initial coalescence phase in standard culture plates directly into custom bioreactors, where the fluid could be confined to flow through the tissue and membrane(s).

In order to form a tissue with depth variations in matrix content and mechanical properties similar to native cartilage, several issues must be addressed. The non-dimensional parameters in this model provide bases for choosing certain boundary conditions and flow parameters to prevent excessive accumulation or loss of molecules near the construct surfaces. For constructs grown without an exogenous scaffold, the design choice of either a single membrane that restricts transport of macromolecules, or a combination of a highly permeable and a restrictive membrane is suggested to generate monotonic proteoglycan variations, similar to articular cartilage. For constructs that attempt to vary mechanical properties with depth by altering the composition of a scaffold, the current model may provide insight into the development of tissue properties after significant culture duration. Constructs formed with chondrocytes seeded in layers of agarose with different concentrations initially exhibited the properties of the agarose, but with time the depth-dependent properties became less dramatic, likely due to metabolic and transport issues (Ng et al. 2005). Current methods of combining specific cells and/or materials in ways expected to

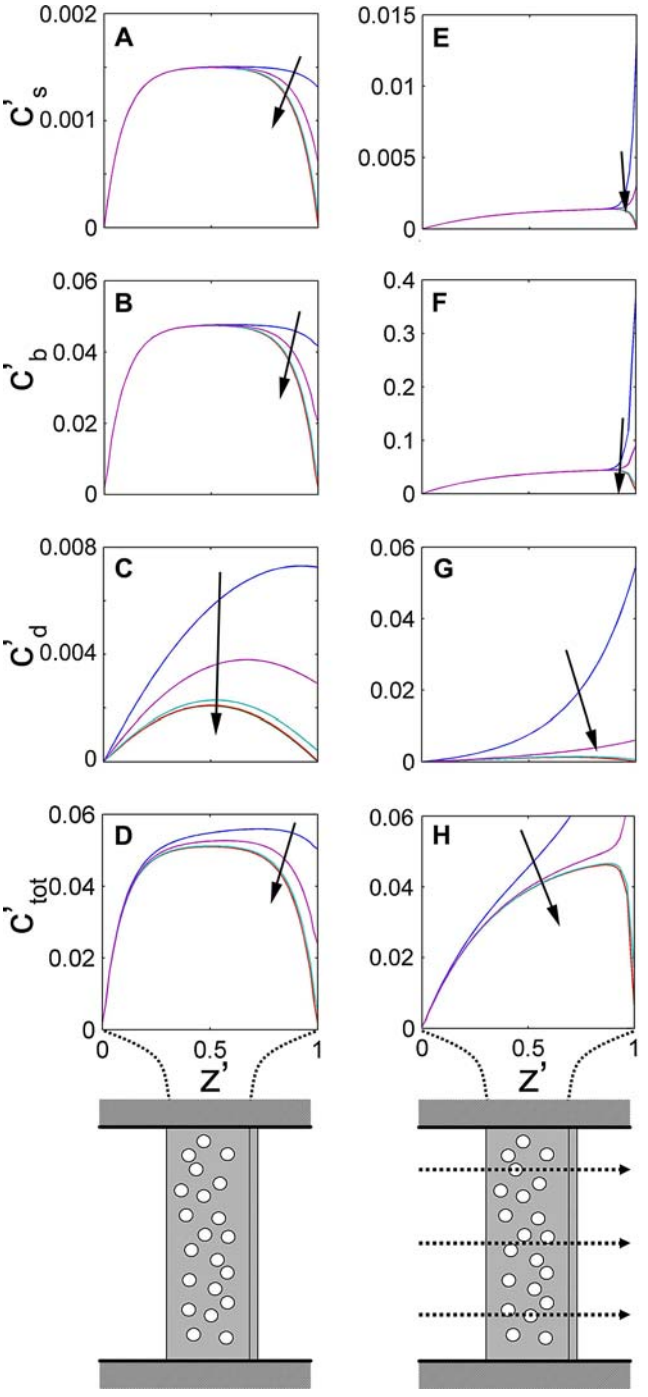

Fig. 5 Equilibrium normalized concentration profiles of soluble, bound, degraded, and total molecules as a function of the non-dimensional membrane parameter, λ_s, which was varied logarithmically from 0.17 to 1.7×10^3 (increasing in the direction of the *arrow*), with $\lambda_s = 10\cdot\lambda_d$. Profiles for constructs cultured **a–d** without perfusion, and **e–h** with perfusion

generate differences in mechanical properties appear not to be sufficient for the long-term maintenance of such properties. Models such as the one described here may help understand the complex regulation of mechanical properties by identifying parameters important for creating specific patterns of matrix accumulation.

Acknowledgements The authors thank Nancy Hsieh for her careful reading of the manuscript. This work was supported by the National Institute of Health, National Science Foundation, and National Aeronautics and Space Administration.

References

Arner EC, Pratta MA, Trzaskos JM, Decicco CP, Tortorella MD (1999) Generation and characterization of aggrecanase. A soluble, cartilage-derived aggrecan-degrading activity. J Biol Chem 274:6594–6601

Blanch HW, Clark DS (1996) Biochemical engineering. Marcel Dekker, New York

Buckwalter JA, Mankin HJ (1997) Articular cartilage. Part I: tissue design and chondrocyte-matrix interactions. J Bone Joint Surg Am 79-A:600–611

Buckwalter JA, Mankin HJ (1998) Articular cartilage: degeneration and osteoarthritis, repair, regeneration, and transplantation. Instr Course Lect 47:487–504

Buschmann MD, Gluzband YA, Grodzinsky AJ, Kimura JH, Hunziker EB (1992) Chondrocytes in agarose culture synthesize a mechanically functional extracellular matrix. J Orthop Res 10:745–758

Chen SS, Falcovitz YH, Schneiderman R, Maroudas A, Sah RL (2001) Depth-dependent compressive properties of normal aged human femoral head articular cartilage. Osteoarthritis Cartilage 9:561–569

Church RL, Pfeiffer SE, Tanzer ML (1971) Collagen biosynthesis: synthesis and secretion of a high molecular weight collagen precursor (procollagen). Proc Natl Acad Sci USA 68:2638–2642

Comper WD, Williams RP (1987) Hydrodynamics of concentrated proteoglycan solutions. J Biol Chem 262:13464–13471

Davisson TH (2001) Biophysical regulation of metabolic balance in tissue engineered articular cartilage. University of California, San Diego, La Jolla

Davisson TH, Sah RL, Ratcliffe AR (2002) Perfusion increases cell content and matrix synthesis in chondrocyte three-dimensional cultures. Tissue Eng 8:807–816

DiMicco MA, Sah RL (2003) Dependence of cartilage matrix composition on biosynthesis, diffusion, and reaction. Transport Porous Med 50:57–73

Dunkelman NS, Zimber MP, LeBaron RG, Pavelec R, Kwan M, Purchio AF (1995) Cartilage production by rabbit articular chondrocytes on polyglycolic acid scaffolds in a closed bioreactor system. Biotechnol Bioeng 46:299–305

Freed LE, Langer R, Martin I, Pellis NR, Vunjak-Novakovic G (1997) Tissue engineering of cartilage in space. Proc Natl Acad Sci USA 94:13885–13890

Galban CJ, Locke BR (1997) Analysis of cell growth in a polymer scaffold using a moving boundary approach. Biotechnol Bioeng 56:422–432

Gooch KJ, Kwon JH, Blunk T, Langer R, Freed LE, Vunjak-Novakovic G (2001) Effects of mixing intensity on tissue-engineered cartilage. Biotechnol Bioeng 72:402–407

Grogan SP, Rieser F, Winkelmann V, Berardi S, Mainil-Varlet P (2003) A static, closed and scaffold-free bioreactor system that permits chondrogenesis in vitro. Osteoarthritis Cartilage 11:403–411

Haddo O, Mahroof S, Higgs D, David L, Pringle J, Bayliss M, Cannon SR, Briggs TW (2004) The use of chondrogide membrane in autologous chondrocyte implantation. Knee 11:51–55

Hascall VC, Luyten FP, Plaas AHK, Sandy JD (1990) Steady-state metabolism of proteoglycans in bovine articular cartilage. In: Maroudas A, Kuettner K (ed) Methods in Cartilage Research. Academic Press, San Diego

Heywood HK, Sembi PK, Lee DA, Bader DL (2004) Cellular utilization determines viability and matrix distribution profiles in chondrocyte-seeded alginate constructs. Tissue Eng 10:1467–1479

Jennings L, Wu L, King KB, Hammerle H, Cs-Szabo G, Mollenhauer J (2001) The effects of collagen fragments on the extracellular matrix metabolism of bovine and human chondrocytes. Connect Tissue Res 42:71–86

Klein TJ (2005) Cartilage tissue engineering: biophysical modulation of functional depth-dependent properties. University of California, San Diego, La Jolla, CA

Klein TJ, Schumacher BL, Schmidt TA, Li KW, Voegtline MS, Masuda K, Thonar EJ-MA, Sah RL (2003) Tissue engineering of articular cartilage with stratification using chondrocyte subpopulations. Osteoarthritis Cartilage 11:595–602

Klisch SM, Chen SS, Sah RL, Hoger A (2003) A growth mixture theory for cartilage with application to growth-related experiments on cartilage explants. J Biomech Eng 125:169–179

Leddy HA, Awad HA, Guilak F (2004) Molecular diffusion in tissue-engineered cartilage constructs: effects of scaffold material, time, and culture conditions. J Biomed Mater Res 70B:397–406

Leddy HA, Guilak F (2003) Site-specific molecular diffusion in articular cartilage measured using fluorescence recovery after photobleaching. Ann Biomed Eng 31: 753–760

Li KW, Klein TJ, Chawla K, Nugent GE, Bae WC, Sah RL (2004) In vitro physical stimulation of tissue-engineered and native cartilage. In: Sabatini M, DeCeuninck F, Pastoureau P (eds) Cartilage and osteoarthritis, vol 100. Humana Press, Totowa, NJ

Masuda K, Sah RL, Hejna MJ, Thonar EJ-MA (2003) A novel two-step method for the formation of tissue engineered cartilage: the alginate-recovered-chondrocyte (ARC) method. J Orthop Res 21:139–148

Mauck RL, Nicoll SB, Seyhan SL, Ateshian GA, Hung CT (2003) Synergistic action of growth factors and dynamic loading for articular cartilage tissue engineering. Tissue Eng 9:597–611

Mauck RL, Soltz MA, Wang CC, Wong DD, Chao PH, Valhmu WB, Hung CT, Ateshian GA (2000) Functional tissue engineering of articular cartilage through dynamic loading of chondrocyte-seeded agarose gels. J Biomech Eng 122:252–260

Menzel A (2005) Modelling of anisotropic growth in biological tissues: a new approach and computational aspects. Biomech Model Mechanobiol 3:147–171

Mizuno S, Tateishi T, Ushida T, Glowacki J (2002) Hydrostatic fluid pressure enhances matrix synthesis and accumulation by bovine chondrocytes in three-dimensional culture. J Cell Physiol 193:319–327

Mow VC, Guo XE (2002) Mechano-electrochemical properties of articular cartilage: their inhomogeneities and anisotropies. Annu Rev Biomed Eng 4:175–209

Mow VC, Wang CC, Hung CT (1999) The extracellular matrix, interstitial fluid and ions as a mechanical signal transducer in articular cartilage. Osteoarthritis Cartilage 7:41–58

Mow VC, Zhu W, Ratcliffe A (1991) Structure and function of articular cartilage and meniscus. In: Mow VC, Hayes WC (eds) Basic orthopaedic biomechanics. Raven Press, New York

Ng KW, Wang CC, Mauck RL, Kelly TN, Chahine NO, Costa KD, Ateshian GA, Hung CT (2005) A layered agarose approach to fabricate depth-dependent inhomogeneity in chondrocyte-seeded constructs. J Orthop Res 23:134–141

Obradovic B, Carrier RL, Vunjak-Novakovic G, Freed LE (1999) Gas exchance is essential for bioreactor cultivation of tissue engineered cartilage. Biotechnol Bioeng 63:197–205

Obradovic B, Meldon JH, Freed LE, Vunjak-Novakovic G (2000) Glycosaminoglycan deposition in engineered cartilage: Experiments and mathematical model. AIChE J 46:1860–1871

Pazzano D, Mercier KA, Moran JM, Fong SS, DiBiasio DD, Rulfs JX, Kohles SS, Bonassar LJ (2000) Comparison of chondrogensis in static and perfused bioreactor culture. Biotechnol Prog 16:893–896

Pei M, Solchaga LA, Seidel J, Zeng L, Vunjak-Novakovic G, Caplan AI, Freed LE (2002) Bioreactors mediate the effectiveness of tissue engineering scaffolds. FASEB J 16:1691–1694

Raimondi MT, Boschetti F, Falcone L, Migliavacca F, Remuzzi A, Dubini G (2004) The effect of media perfusion on three-dimensional cultures of human chondrocytes: integration of experimental and computational approaches. Biorheology 41:401–410

Riesle J, Hollander AP, Langer R, Freed LE, Vunjak-Novakovic G (1998) Collagen in tissue-engineered cartilage: types, structure, and crosslinks. J Cell Biochem 71:313–327

Sah RL, Chen AC, Grodzinsky AJ, Trippel SB (1994) Differential effects of IGF-I and bFGF on matrix metabolism in calf and adult bovine cartilage explants. Arch Biochem Biophys 308:137–147

Sah RL, Klein TJ, Schmidt TA, Albrecht DR, Bae WC, Nugent GE, McGowan KB, Temple MM, Jadin KD, Schumacher BL, Chen AC, Sandy JD (2004) Articular cartilage repair, regeneration, and replacement. In: Koopman WJ (ed) Arthritis and allied conditions: A Textbook of rheumatology. Lippincott Williams & Wilkins, Philadelphia

Sandy JD, O'Neill JR, Ratzlaff LC (1989) Acquisition of hyaluronate-binding affinity in vivo by newly synthesized cartilage proteoglycans. Biochem J 258:875–880

Sandy JD, Plaas AHK (1986) Age-related changes in the kinetics of release of proteoglycans from normal rabbit cartilage explants. J Orthop Res 4:263–272

Schinagl RM, Gurskis D, Chen AC, Sah RL (1997) Depth-dependent confined compression modulus of full-thickness bovine articular cartilage. J Orthop Res 15:499–506

Smith RL, Carter DR, Schurman DJ (2004) Pressure and shear differentially alter human articular chondrocyte metabolism: a review. Clin Orthop S89–s95

Smith RL, Donlon BS, Gupta MK, Mohtai M, Das P, Carter DR, Cooke J, Gibbons G, Hutchinson N, Schurman DJ (1995) Effects of fluid-induced shear on articular chondrocyte morphology and metabolism in vitro. J Orthop Res 13:824–831

Trindade MC, Shida J, Ikenoue T, Lee MS, Lin EY, Yaszay B, Yerby S, Goodman SB, Schurman DJ, Smith RL (2004) Intermittent hydrostatic pressure inhibits matrix metalloproteinase and pro-inflammatory mediator release from human osteoarthritic chondrocytes in vitro. Osteoarthritis Cartilage 12:729–735

Vunjak-Novakovic G, Obradovic B, Martin I, Freed LE (2002) Bioreactor studies of native and tissue engineered cartilage. Biorheology 39:259–268

Wilson CG, Bonassar LJ, Kohles SS (2002) Modeling the dynamic composition of engineered cartilage. Arch Biochem Biophys 408:246–254

Yellowley CE, Jacobs CR, Donahue HJ (1999) Mechanisms contributing to fluid-flow-induced Ca^{2+} mobilization in articular chondrocytes. J Cell Physiol 180:402–408